

Predictions of Optical Excitations in Transition-Metal Complexes with Time Dependent-Density Functional Theory: Influence of Basis Sets

Laurence Petit,^{†,‡} Pascale Maldivi,[†] and Carlo Adamo^{*,‡}

Laboratoire de Reconnaissance Ionique, DRFMC/LCIB (UMR_E 3 CEA-UJF), CEA-Grenoble, 17 rue des Martyrs, F-38054 Grenoble Cedex 9, France, and Laboratoire d'Électrochimie et de Chimie Analytique, CNRS UMR-7575, École Nationale Supérieure de Chimie de Paris, 11 rue P. et M. Curie, F-75231 Paris Cedex 05, France

Received March 2, 2005

Abstract: The calculation of the absorption spectra of four families of transition-metal complexes ($\text{Ni}(\text{CO})_4$, MnO_4^- , MF_6 ($\text{M} = \text{Cr}, \text{Mo}, \text{W}$) and $\text{CpM}(\text{CO})_2$ ($\text{M} = \text{Rh}, \text{Ir}$)) has been undertaken to unravel the influence of basis sets onto excitation energies, oscillator strengths, and assignments. Three among the most common pseudopotentials, with the corresponding valence basis sets, and two all-electron basis sets have been used for the metal center description in the framework of the time dependent Density Functional Theory (TD-DFT). Our results show that this approach does not particularly depend on the basis set used on the metal atoms. Furthermore, the chosen functional PBE0 provides transitions in good agreement with experiments, and it provides an accuracy of about 0.3 eV, comparable to that of refined post-Hartree–Fock methods.

1. Introduction

Over the past three decades, numerous computational strategies have been developed for the simulation of electronic spectra. In particular, electronic properties of transition-metal complexes have been of great interest due to the chemical relevance of such systems in many fields from medicine^{1,2} to material design.^{3,4} In this perspective, theoretical approaches rooted in quantum chemistry obviously present numerous advantages and have notably helped a lot in clarifying experimental spectra or in assessing solvent-related properties. Yet, available tools are often time-demanding, and, overall, they require a careful choice of the computational parameters. Both points can be a major problem when dealing with large systems of chemical interest.

Theoretical methods based on the Density Functional Theory (DFT), which combine both speed and accuracy, have thus been widely used in this field.⁶ In particular, the so-called time dependent DFT (TD-DFT) approach has become

a key method validated in numerous works on organic and bioorganic compounds^{6–8} as well as on metal complexes.^{2,9,10} Based on the linear response theory, it enables to calculate molecular properties such as polarizabilities^{11,12} and excitation energies^{6–10} by applying a time-dependent field to the system and analyzing its dynamic response.¹³ Another main advantage of TD-DFT methods rests on their lack of preliminary assumption concerning the molecular orbitals involved in excitations. This point is of particular relevance when the nature of the excited state is unknown and cannot be clearly deduced from experiments.^{9,14}

Even though it is easily accessible, some cares, relative to the functional and basis sets used, must be taken. The first point, i.e., functional assessment, has been deeply discussed in the literature. In particular, it has been shown that large discrepancies are notably caused by the incorrect asymptotic behavior of the approximated functionals and by the self-interaction error (SIE).^{15,16} Various strategies have been proposed to overcome this failure, such as asymptotically corrected potentials^{17,18} or by including the Hartree–Fock potential at long-range.¹⁹ More easily, the hybrid approach that introduces some HF exact exchange can

* Corresponding author e-mail: carlo-adamo@enscp.fr.

[†] DRFMC/SCIB.

[‡] École Nationale Supérieure de Chimie de Paris.

Table 1. Contraction Schemes for the All Electron and Valence Basis Sets Considered in the Present Paper

atom	LANL2DZ	SBKJC	SDD	DZVP	Watchers + f
Ni	(5s,5p,5d)/[3s,3p,2d]	(8s,8p,6d)/[4s,4p,3d]	(8s,7p,6d,1f)/[6s,5p,3d,1f]	(15s, 9p,5d)/[5s,3p,2d]	(14s,11p,6d,3f)/[8s,6p,4d,1f]
Mn	(5s,5p,5d)/[3s,3p,2d]	(8s,8p,6d)/[4s,4p,3d]	(8s,7p,6d,1f)/[6s,5p,3d,1f]	(15s, 9p,5d)/[5s,3p,2d]	(14s,11p,6d,3f)/[8s,6p,4d,1f]
Cr	(5s,5p,5d)/[3s,3p,2d]	(8s,8p,6d)/[4s,4p,3d]	(8s,7p,6d,1f)/[6s,5p,3d,1f]	(15s, 9p,5d)/[5s,3p,2d]	
Mo	(5s,6p,4d)/[3s,3p,2d]	(7s,7p,5d)/[4s,4p,3d]	(8s,7p,6d)/[6s,5p,3d]	(18s,12p,9d)/[6s,5p,3d]	
W	(8s,6p,3d)/[3s,3p,2d]	(7s,7p,5d)/[4s,4p,3d]	(8s,7p,6d)/[6s,5p,3d]		
Rh	(5s,6p,4d)/[3s,3p,2d]	(7s,7p,5d)/[4s,4p,3d]	(8s,7p,6d)/[6s,5p,3d]	(18s,12p,9d)/[6s,5p,3d]	
Ir	(8s,6p,3d)/[3s,3p,2d]	(7s,7p,5d)/[4s,4p,3d]	(8s,7p,6d)/[6s,5p,3d]		

represent an interesting alternative. Among others, the PBE0 hybrid functional^{20,21,27} has many times proved its efficiency on a wide range of compounds, and it generally provides accurate results on ground and excited-state properties, including charge-transfer transitions.^{6,22–26} It derives from the Perdew-Burke-Erzenrhof PBE exchange-correlation functional,²⁷ but it is not fitted on any experimental data. In contrast, at the best of our knowledge, the dependence of the TD-DFT approach on basis sets has never been systematically tested for metal-containing complexes. It is nevertheless well-known that basis sets can affect molecular properties, including excited states.^{28,29}

To elucidate this point, often not well explored in TD-DFT applications, we have considered in the present study several benchmark cases, combining simple structure, various ligands and metals. The chosen metal complexes have been well characterized at both experimental and theoretical levels so as to allow detailed comparisons. We have thus worked out the absorption spectra of four classes of transition-metal complexes: Ni(CO)₄, MnO₄[−], MF₆ (M = Cr, Mo, W) and CpM(CO)₂ (M = Rh, Ir). Their spectra have been computed using different pseudopotentials, selected among those commonly used in TD-DFT applications^{30,31} as well as of two all-electron basis sets, especially developed for metals.

2. Computational Details

All calculations were performed with the Gaussian 03 package.³² Optimizations were carried out at the DFT level of theory, while absorption spectra were computed as vertical electronic excitations from the ground state using the TD-DFT approach as implemented in Gaussian.³³ For both types of calculations, the PBE0 hybrid functional,^{20,21} that includes 25% of exact exchange, was used. All systems were studied in their highest symmetry, that is *T_d* for Ni(CO)₄ and MnO₄[−],^{34–36} *O_h* symmetry for MF₆ complexes (M = Cr, Mo, W)^{37–41} and *C_s* for CpM(CO)₂ (M = Rh, Ir).⁴² Even though the correct symmetry of CrF₆, and even its very existence, are still a source of controversy, recent studies tend to favor the *O_h* group.^{37–39}

Three different pseudopotentials, namely those of Hay, Wadt, and co-workers (LANL2DZ^{43,44}), those of Stevens and co-workers (SBKJC⁴⁵), and those of the Stuttgart group (SDD^{46,47}), with the corresponding valence basis sets are herein considered. Two all-electron basis sets were also used: the “classical” basis of Watchers,^{48,49} including a *f* diffuse function, and the more recent DZVP for DFT calculations, either from Chiodo and co-workers⁵⁰ or Godbout et al.⁵¹ All the considered basis and contraction schemes are

summarized in Table 1. Whatever the complex is, remaining atoms (F, O, C, and H) were always described with the 6-31+G(2d,p) basis set as suggested by Daniel.⁵²

3. Results and Discussion

We want to add few general remarks concerning our calculations before discussing them. On one hand, only the best results are discussed in details for a given system, while, for other basis sets, the sole transitions with experimental counterparts are reported in the tables. Each time, contributions to a given transition having participations below 5% are not mentioned. On the other hand, all the TD-DFT calculations have been carried out on the optimized structure with the above-mentioned criteria. We have nonetheless checked that results starting from X-ray structures were similar, with maximum discrepancies in the order of 10 nm. Since significant differences were observed only for the permanganate ion, both sets of transitions are reported in this case. On the whole, optimized geometries, reported in the Supporting Information (see Table SI), are quite close to the experimental values. Finally, we only focused on spin-allowed transitions, i.e., singlet excitations.

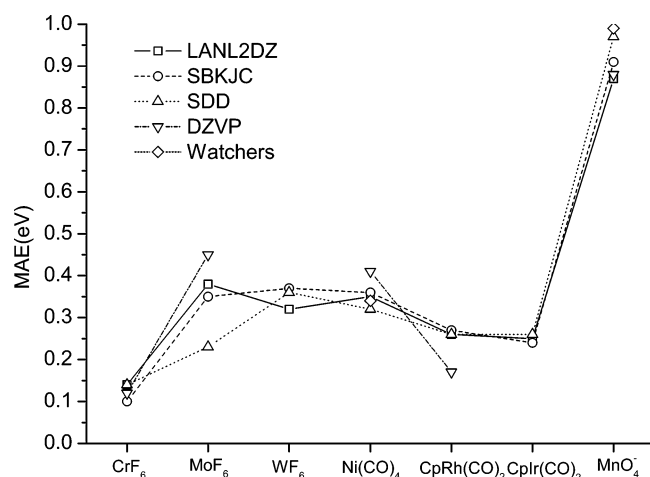
MF₆, M = Cr, Mo, W. We have chosen as the first tests three extensively studied hexafluoride complexes, namely CrF₆, MoF₆, and WF₆. Such systems are formally M(VI) complexes and the metal atoms have a d⁰ electronic configuration. Indeed, all the valence occupied orbitals have essentially ligand character, while the first unoccupied orbitals are centered on the metal. Transitions are thereby expected to be essentially made of ligand to metal charge transfer (LMCT). Moreover, despite numerous controversies,^{53–55} the octahedral geometry was adopted for the three systems. The only spin and symmetry allowed excitations are thus ¹A_{1g} → ¹T_{1u} transitions. The fluorides generate a strong crystal field that increases in going from Cr to W. The metal e_g orbitals are thus quite high in energy, and most of the absorption bands are to t_{2g} levels. As expected, CrF₆, MoF₆, and WF₆ spectra are akin in relative structure, intensities, and assignments. In particular, three allowed charge-transfer bands are recorded whatever the complex is. For MoF₆ and WF₆, they go with several dipole-forbidden transitions lying high in energy and consequently ascribed to Rydberg states.

On the whole, our results are in very good agreement with available experimental data,^{56,57} as shown in Table 2. The mean absolute errors (MAE) on energies are rather low, ranging from 0.43 eV for WF₆ (LANL2DZ), 0.23 eV for MoF₆ (SDD), to 0.10 eV for CrF₆ (SBKJC). What is more,

Table 2. Excitation Energies (eV), Oscillator Strengths, and Corresponding Assignments Calculated on the PBE0 Structure of CrF₆, MoF₆, and WF₆^c

PBE0			theoretical reference ^a			experiment ^b		
excitation energy	oscillator strength	assignments	excitation energy	oscillator strength	assignments	excitation energy	oscillator strength	assignments
CrF ₆ (SBKJC ECP)								
3.13	0.0018	79%(t _{1u} →t _{2g}) + 21%(t _{2u} →t _{2g})	2.38	0.0002	(t _{1u} →t _{2g}) + (t _{2u} →t _{2g})	3.31	middle	
3.89	0.0272	60%(t _{2u} →t _{2g}) + 35%(t _{1u} →t _{2g}) + 5%(t _{1u} →e _g)	3.12	0.0138	(t _{1u} →t _{2g}) + (t _{2u} →t _{2g})	3.88	strong	
4.89	0.0273	76%(t _{1u} →t _{2g}) + 18%(t _{1u} →e _g) + 6%(t _{2u} →t _{2g})	4.21	0.0406	(t _{1u} →t _{2g}) + (t _{2u} →t _{2g})	4.77	strong	
MoF ₆ (SDD)								
5.51	0.0028	85%(t _{1u} →t _{2g}) + 15%(t _{2u} →t _{2g})	5.55	0.0243	100%(t _{1u} →t _{2g})	5.90	weak	t _{1g} →t _{2g}
6.03	0.0197	51%(t _{1u} →t _{2g}) + 49%(t _{2u} →t _{2g})	6.62	0.0945	100%(t _{2u} →t _{2g})	6.54	middle	t _{1u} →t _{2g}
7.15	0.1618	60%(t _{1u} →t _{2g}) + 27%(t _{2u} →t _{2g}) + 13%(t _{1u} →e _g)	7.24	0.3549	100%(t _{1u} →t _{2g})	7.12	strong	t _{2u} →t _{2g}
8.71	forbidden	100%(e _g →t _{2g})	8.91	forbidden	100%(t _{2g} →t _{2g})	8.62	very weak	e _g →t _{2g}
9.08	forbidden	100%(e _g →t _{2g})	9.49	forbidden	100%(e _g →t _{2g})	9.22	very weak	e _g →t _{2g}
WF ₆ (LANL2DZ)								
6.72 (184.60)	0.0028	82%(t _{1u} →t _{2g}) + 18%(t _{2u} →t _{2g})	7.20	t _{1g} →t _{2g}		7.23	weak	t _{1g} →t _{2g}
7.22 (171.79)	0.0280	54%(t _{1u} →t _{2g}) + 46%(t _{2u} →t _{2g})	7.92	t _{1u} →t _{2g}		8.05	middle	t _{2u} →t _{2g}
8.34 (148.72)	0.2193	60%(t _{1u} →t _{2g}) + 29%(t _{2u} →t _{2g}) + 11%(t _{1u} →e _g)	8.68	t _{1u} →t _{2g}		8.60	strong	t _{1u} →t _{2g}
9.05 (136.97)	forbidden	100%(t _{2g} →t _{2g})	9.07	a _{1g} →t _{2g}		8.94	very weak	t _{1u} →t _{2g}
10.18 (121.78)	forbidden	100%(e _g →t _{2g})				10.03	very weak	a _g →t _{2g}
11.11 (111.61)	forbidden	80%(t _{2g} →t _{2g}) + 20%(e _g →t _{2g})				11.05	very weak	e _g →t _{2g}

^a Theoretical references: TD-DFT for CrF₆ (ref 60), SAC-CI for MoF₆ (ref 58), and X α method for WF₆ (ref 59). ^b Experimental references: ref 56 for CrF₆ in N₂ matrix, ref 57 for MoF₆ and WF₆ in gaseous phase. ^c The reported results are those in better agreement with the experiments, and they have been obtained with different pseudopotentials for the metal atoms.

**Figure 1.** Mean absolute errors (MAEs, eV) for the vertical transitions of CrF₆, MoF₆, WF₆, Ni(CO)₄, CpRh(CO)₂, CpIr(CO)₂, and MnO₄⁻ complexes, computed using different pseudopotentials and related valence basis sets (LANL2DZ, SBKJC, SDD) as well as the DZVP and Watchers+*f* all-electron basis.

this discrepancy is almost constant from one basis set to another, as can be seen from the MAEs reported in Figure 1. MoF₆ seems however not to respect this trend since wide variations are observed from SDD (MAE of 0.23 eV) to DZVP (MAE of 0.45 eV) with intermediate MAE for LANL2DZ (0.38 eV) and SBKJC (0.35 eV). In any cases, the largest deviations (around 0.4/0.5 eV) are for the first two lowest excitations that can be assigned as LMCT

transitions. These errors are nonsystematic, so that the nonsystematic trends can be clearly evidenced. Therefore it is difficult to argue that these deviations are related to the limits of the basis considered or to an intrinsic problem to the TD-DFT method when dealing with charge-transfer transitions.¹⁶

Intensities are well reproduced, with an increasing pattern from the first allowed band to the last one. In contrast, theoretical assignments are more questionable when compared to experimental suggestions. As illustrated by the MoF₆ complex, all our bands with the exception of the first one are consistent with the experiment, but several transitions display some interconfigurational mixing. Actually, different assignments have been proposed for the transitions of MoF₆,^{23,57–59} leading to some inconsistencies. For instance, as previously revealed by Nakai and co-workers⁵⁸ the experimental assignment of the first band is arguable since t_{1g}→t_{2g} transitions are calculated at lower energies (4.91 and 5.01 eV in our work) and are forbidden (see Table SII, Supporting Information). On the other hand, beyond 7.5 eV, all the transitions are forbidden with close assignments. A rigorous analysis with respect to experiment can thus turn out to be difficult.

It is nevertheless important to highlight the accuracy of our results with respect to other theoretical calculations. With the exception of WF₆ whose absorption spectrum is particularly accurate at the X α level,⁵⁹ results on MoF₆ and CrF₆ are at least comparable or even better than in previous SAC-CI⁵⁷ and TD-DFT calculations, respectively.⁶⁰ In particular, CrF₆ needs some comments. In fact, previous calculations,⁶⁰

Table 3. Excitation Energies (eV), Oscillator Strengths, and Corresponding Assignments Calculated with the SDD Pseudopotential on the PBE0 Optimized Structure of Ni(CO)₄

PBE0			CASPT2/CASSCF ^a			experiment ^b excitation energy;
excitation energy	oscillator strength	assignments	excitation energy	oscillator strength	assignments	
4.87	0.0242	82%(t ₂ →t ₂) + 18%(t ₂ →e)	4.34	0.29	92%(t ₂ →t ₂)	4.5, 4.54
5.12	0.0760	72%(t ₂ →e) + 15%(t ₂ →t ₂) + 7%(t ₂ →t ₁) + 6%(e→t ₂)	5.22	0.38	92%(t ₂ →e)	5.4, 5.17, 5.24
5.88	0.0057	76%(e→t ₂) + 21%(t ₂ →t ₁)	5.57	0.29	94%(e→t ₂)	5.52
6.41	0.1700	69%(t ₂ →t ₁) + 16%(e→t ₁) + 12%(e→t ₂)	6.28	0.47	93%(t ₂ →t ₁)	6.0, 6.02
6.68	0.0274	100%(t ₂ →a ₁)				
7.50	0.2721	94%(e→t ₁) + 6%(t ₂ →t ₁)	6.97	0.83	88%(e→t ₁) + 6%(t ₂ →t ₁)	
7.65	0.0189	100%(t ₂ →t ₂)				

^a Reference 64. ^b Reference 63 (gas phase); ref 62 (matrix); ref 61 (solvent).

carried out with a similar approach, did not achieve accurate results as can be seen from the values reported in Table 2. Depending on the used functional, the discrepancy could be attributed either to geometrical problems (LB94) or to a small basis sets (B3LYP calculations).

Ni(CO)₄. Nickel tetracarbonyl is a d¹⁰ system. No d–d transitions are therefore observed, and excitations are dominated by charge transfer. It is an interesting system in our study since three different experimental spectra are available, recorded in solution,⁶¹ in matrix,⁶² and in the gas phase.⁶³ Several calculations at different levels of theory have been performed subsequently.^{64–68} This large amount of results allows an accurate assessment of our work. Experimentally, Ni(CO)₄ features four main transitions. Both solution and gas-phase spectra give a main band around 6 eV with two shoulders at 5.52 and 4.54 eV in solution and 5.4 and 4.5 eV in the gas phase. Only two transitions at 5.17 and 4.54 eV are instead reported in a matrix. These energies, listed in Table 3, are compared to our results calculated with the SDD pseudopotential for the metal center. CASPT2 values,⁶⁴ which are among the most accurate results ever calculated for Ni(CO)₄, are also given. We refer the reader to refs 65 and 51 for a deeper scrutiny of other theoretical methods. According to the Laporte's rule, the system, optimized in *T_d* symmetry, can only present ¹A₁→¹T₂ allowed transitions. Seven of such excitations are listed in Table 3, the four first corresponding to the experimental ones. All the transitions are overestimated, and the MAE is of about 0.3 eV with a maximum deviation of 0.4 eV for the highest transition. Previous TD-DFT calculations performed with the BP functional⁶⁶ show the opposite trend (underestimation) but are nevertheless consistent with our work. As expected, the expensive CASPT2 approach is in better agreement with the experimental values, the MAE being of 0.17 eV.⁶⁴ Turning to intensities, it must be noticed that the experimental trend in solution is respected, the strongest transition being around 6.5 eV (*f* = 0.170) with the two lowest counterparts at 5.12 eV (*f* = 0.076) and 4.87 eV (*f* = 0.024). Oscillator strengths calculated by Pierloot et al.⁶⁴ behave in the same way as ours but are more intense. Nevertheless, it must be noticed that the CASPT2 method does not enable to calculate transition moments and configurations so the values reported in Table 3 originate from a CASSCF calculation.

Orbitals from HOMO-3 to LUMO+3 are calculated to have t₂ symmetry. The last occupied orbitals are essentially

made of Ni 3d orbitals, but some bonding character with the carbonyls is nevertheless observed. The first LUMOs clearly show an antibonding character between the 3d(Ni) and the π*(CO). The four first allowed transitions can be therefore ascribed to charge transfer from the 3d orbitals of nickel to the π*(CO), resulting in a destabilization of the carbonyl. Even so, the assignment of such transitions is still a source of controversy. As previous CASPT2 (assignments made on the basis of CASSCF results, Table 3) and TD-DFT works,^{64,66} we found the allowed bands I to IV to be mainly composed of t₂→t₂, t₂→e, e→t₂, and t₂→t₁ transitions, respectively. Our assignments are in very good agreement with CASSCF calculations and turned out to present less interconfigurational mixing than previous TD-DFT and SAC-CI studies.^{65,66} One can also notice that the excitation at 6.68 eV is not reported in other theoretical works. The CASSCF and TD-DFT calculations only quote one e→t₁ transition, whereas no transition above 5.8 eV appears at the SAC-CI level. This latter excitation is herein found at 7.50 eV and is the most intense one. Actually, as underlined by van Gisbergen et al.,⁶⁶ these differences are difficult to rationalize since they strongly depend on the size of the active space considered in the CASSCF or SAC-CI calculation. In this manner, some orbitals do not appear simply because they are not included at the beginning, as some a₁ orbitals for instance.

The variations observed in going from one basis set to another are quite small. Whatever the basis set considered on the metal center is, Ni–C and C–O bonds are always strengthened by the PBE0 optimization, being on average 0.018 Å too low (see Table SI, Supporting Information). We checked, at the same level of theory with SDD pseudopotential, that this discrepancy did not significantly alter the absorption spectrum, the maximum difference being of a few nanometers. Excitation values for the considered basis sets are all listed in Table 4. Results globally indicate that the way the metal center is described hardly affects the spectrum, the pseudopotentials providing as accurate results as all-electron basis sets. Core electrons have indeed little effect on results since they do not participate in the excitation process. In contrast, the way 3d orbitals of the Ni are described can have a great influence. Furthermore, since the process consists of a charge transfer, polarization or diffuse functions should at least in principle be considered. Yet, discrepancies are herein too small to draw any conclusion.

Table 4. Allowed Transitions of Ni(CO)₄ (in eV) Computed with Different Pseudopotentials and All-Electron Basis Sets^a

LANL2DZ		SBKJC		SDD		DZVP		Watchers + f	
excitation energy	oscillator strength	excitation energy	oscillator strength	excitation energy	oscillator strength	excitation energy	oscillator strength	excitation energy	oscillator strength
4.93	0.0259	4.94	0.0253	4.87	0.0242	5.04	0.0207	4.92	0.0249
5.19	0.0763	5.19	0.0742	5.12	0.0760	5.29	0.0800	5.15	0.0724
5.95	0.0035	5.96	0.0028	5.88	0.0057	6.07	0.0013	5.93	0.0026
6.45	0.1836	6.47	0.1826	6.41	0.1700	6.54	0.1868	6.42	0.1791
6.91	0.0268	6.94	0.0273	6.68	0.0274	6.99	0.0273	6.91	0.0251
7.49	0.0036	7.57	0.2922	7.50	0.2721	7.63	0.2961	7.51	0.2988

^a Assignments being very close from one basis set to another one, they are not mentioned herein.

CpM(CO)₂, M = Rh, Ir. CpM(CO)₂ systems, M = Rh, Ir, have recently been of much interest because they are able to activate the normally unreactive C–H bond when excited.^{69–71} Their absorption spectra is herein studied with three pseudopotentials (LANL2DZ, SBKJC, and SDD) and the DZVP all electron basis set for the rhodium complex. The DZVP results for CpRh(CO)₂ are compared with recent theoretical data at the SAC-CI level of theory⁴² as well as with the few available experimental values⁷² (see Table 5). Note that the SAC-CI assignments are based on our symmetry orientation, as given by the Gaussian program, so as to make comparisons easier. The optimized structures in C_s symmetry are found to have an ¹A' ground state, in agreement with ref 42. Whatever the basis set on the metal center is, the geometry is quite consistent with the SAC-CI one, with the exception of the d(Rh–Cp) distance that is calculated to be on average 0.16 Å too low. Likewise, frontier orbitals are similar.⁴² The last occupied levels (from HOMO-4 to HOMO-1) are dominated by the 4d orbitals of rhodium, while the first unoccupied ones (from LUMO+1 to LUMO+4) present an important antibonding character between d(Rh) and π*(CO). As a consequence, the overall good agreement with these theoretical values is not surprising. Only one significant inversion in the assignments can be observed. These orbitals are mainly involved in two MLCT transitions calculated at 4.43 eV and 4.68 eV (see Table 5). At the SAC-CI level, they are found at 4.38 and 4.45 eV, respectively, after another intense band at 4.36 eV (*f* = 0.1003). This last transition originates from a HOMO to LUMO excitation and corresponds to a charge transfer from Cp to Rh and CO.

More remarkably, in our work, three of the most intense bands lie in the range of 5.7–6.0 eV, namely at 5.75 eV (7A', *f* = 0.1079), 5.82 eV (8A', *f* = 0.0277), and 5.93 eV (9A', *f* = 0.1100). None of these bands appears in the SAC-CI results because these calculations are limited to the four first A' and A'' singlet excitations. They correspond to excitations from the HOMO toward the Cp ligand (for 8A' and 9A') and the carbons of carbonyls (7A').

Results with pseudopotentials are very similar in the band positions, wavelengths, and intensities, except for the highest energies. The graph of Figure 1 well underlines this homogeneity. The three pseudopotentials behave in the same way up to 5 eV, with a small overestimation of excitation energies of about 0.1–0.2 eV with respect to the DZVP values. For instance, the MLCT transitions with LANL2DZ pseudopotential are found to be at 4.60 and 4.79 eV instead

of 4.43 and 4.68 eV. Intensities and orbitals are also akin to the SAC-CI ones. In contrast, when going to high energies, discrepancies are more marked, with states inversions, decreases in intensities, and changes in assignments. More in details, 7A', 8A', and 9A' intense states calculated with the DZVP basis set appear to be weaker, whereas forbidden A'' excitations become allowed. Such differences are quite puzzling. Actually, in Hu et al.⁴² SAC-CI study, metals are described by the Hay–Wadt relativistic effective pseudopotential⁷³ that has almost the same characteristics as ours (28 core electrons, (5s,6p,4d) → [3s,3p,2d] for Rh). The observed difference between our results with pseudopotentials and the SAC-CI ones is thus a matter of methodology. When using the all-electron DZVP basis set, results become surprisingly better, whereas no relativistic effect is taken into account. Presumably, this behavior depends on error compensation.

The calculated excitation energies, oscillator strengths, and assignments for the CpIr(CO)₂ complex with LANL2DZ, SBKJC, and SDD pseudopotentials are shown in Table 6. On the whole, they are very close to the ones with rhodium, except for high energies transitions and for small differences in assignments. Yet, since the DZVP basis set is not available, they are not more accounted for herein. One should notice that the comparison with SAC-CI results is not complete because of problems of assignments.

MnO₄[−] The permanganate ion is a very challenging system because it involves both configuration mixing in excitations and important correlation effects. For this reason, numerous theoretical works have been dedicated to the study of its absorption spectrum with a wide range of methods, from ΔSCF⁷⁴ to CI(SD).⁷⁵ Yet, lots of inconsistencies in energies and assignments appear. A CASPT2 multiconfigurational treatment is difficult since a large active space would be necessary. A SAC-CI study⁷⁶ has nevertheless managed to calculate energies in quite good agreement with experimental data. Our results, based on the optimized tetrahedral structure with LANL2DZ pseudopotential for singlet excitation energies, oscillator strengths, and assignments, are listed in Table 7. They are compared to the experimental values recorded by Holt and co-workers.⁷⁷ As expected for a d⁰ complex, we found the last occupied levels to be mainly composed of p(O) orbitals, while the first unoccupied levels mix 3d orbitals of manganese and p orbitals of oxygen. In this manner, the allowed bands correspond to LMCT bands. In agreement with other theoretical works,^{60,66,76} the lowest allowed band is ascribed to a t₁→e transition at 3.08 eV.

Table 5. Excitation Energies (eV), Oscillator Strengths, and Assignments Calculated with the DZVP Basis Set on the PBE0 Optimized Structure of CpRh(CO)₂

PBE0				SAC-CI ^a				experiment ^b excitation energy
state	excitation energy	oscillator strength	assignments	state	excitation energy	oscillator strength	assignments	
1A''	2.73	forbidden	100%(34a'→21a'')	1A''	2.71	forbidden	57%(34a'→36a') + 29%(34a'→35a') + 7%(19a''→36a')	2.93
2A''	3.55	0.0050	100%(33a'→21a'')	2A''	3.22	0.0081	64%(33a'→36a') + 25%(33a'→35a')	
1A'	3.93	forbidden	95%(34a'→36a') + 5%(19a''→21a'')	1A'	3.95	forbidden	61%(20a''→36a') + 24%(20a''→35a') + 7%(34a'→28a'')	
2A'	4.36	0.1003	86%(34a'→35a') + 9%(20a''→21a'')	4A'	4.57	0.1671	67%(34a'→21a'') + 24%(34a'→22a'') + 9%(34a'→23a'')	
3A'	4.43	0.0021	79%(19a''→21a'') + 14%(33a'→35a')	2A'	4.38	0.0116	31%(33a'→22a'') + 29%(33a'→21a'') + 24%(34a'→23a'') + 16%(34a'→22a'')	4.34
3A''	4.59	forbidden	97%(34a'→23a'')					
4A'	4.68	0.0095	89%(33a'→35a') + 11%(19a''→21a'')	3A'	4.45	0.0359	34%(33a'→22a'') + 34%(33a'→21a'') + 19%(34a'→23a'') + 13%(33a'→23a'')	
4A''	4.90	0.0227	66%(34a'→22a'') + 34%(32a'→21a'')					
5A'	4.97	0.0007	97%(33a'→36a')					
5A''	5.14	0.0147	65%(32a'→21a'') + 24%(34a'→22a'') + 7%(32a'→23a'')	3A''	4.84	0.0045	61%(32a'→36a') + 24%(32a'→35a')	
6A'	5.20	forbidden	100%(34a'→37a')					
6A''	5.48	forbidden	100%(33a'→22a'')					
7A''	5.65	0.0051	49%(33a'→23a'') + 31%(31a'→21a'') + 11%(34a'→24a'')	4A''	5.86	0.0012	28%(34a'→36a') + 28%(19a''→36a') + 24%(19a''→35a') + 20%(34a'→35a')	
8A''	5.65	0.0005	53%(33a'→23a'') + 32%(31a'→21a'') + 12%(34a'→24a'')					
7A'	5.75	0.1079	70%(34a'→38a') + 17%(20a''→21a'') + 9%(34a'→39a')					
9A''	5.75	forbidden	70%(34a'→24a'') + 9%(34a'→25a'') + 8%(19a''→35a') + 8%(31a'→21a'')					
10A''	5.79	0.0014	59%(19a''→35a') + 17%(34a'→25a'') + 11%(31a'→21a'') + 8%(34a'→24a'')					
8A'	5.82	0.0277	54%(34a'→39a') + 28%(34a'→38a') + 14%(34a'→40a')					
11A''	5.88	forbidden	79%(19a''→36a') + 12%(31a'→21a'') +					
9A'	5.93 (209.23)	0.1100	43%(34a'→39a') + 26%(34a'→40a') + 23%(20a''→21a'') + 6%(34a'→38a')					

^a Reference 42. ^b In decalin, ref 72.

This energy is upshifted of 0.8 eV with respect to the experimental excitation. A similar trend is found for the other bands, the largest difference being about 1 eV. In contrast,

oscillator strengths behave in the same way as the experimental spectrum. The third band is indeed the most intense, with another first strong excitation and a weak one at 4.31

Table 6. Excitation Energies (eV), Oscillator Strengths, and Assignments Calculated with LANL2DZ Pseudopotential on the Optimized Structure of $\text{CpIr}(\text{CO})_2^b$

PBE0				SAC-CI ^a			
state	excitation energy	oscillator strength	assignments	state	excitation energy	oscillator strength	assignments
1A''	3.57	forbidden	100%(24a'→17a'')	1A''	3.30	forbidden	50%(23a'→17a'') + 50%(23a'→25a')
2A''	4.40	0.0042	100%(23a'→17a'')	2A''	3.84	0.0073	53%(16a''→25a') + 47%(16a''→17a'')
1A'	4.43	forbidden	78%(24a'→25a') + 9%(24a'→27a') + 7%(24a'→26a')	1A'	4.55	0.0002	38%(23a'→27a') + 25%(15a''→25a') + 19%(15a''→17a'')
2A'	4.97	0.1318	82%(24a'→26a') + 9%(24a'→25a')	3A'	5.00	0.2132	73% (23a'→24a') + 27%(23a'→18a'')
3A''	5.04	0.0003	54%(24a'→19a'') + 37%(24a'→20a'') + 9%(24a'→18a'')	3A''	5.15	0.0001	
4A''	5.18	0.0094	83%(24a'→18a'') + 7%(22a'→17a'') + 6%(24a'→19a'')				
3A'	5.19	0.0064	64%(23a'→26a') + 19%(16a''→17a'') + 8%(23a'→25a') + 5%(23a'→28a')	2A'	4.93	0.0335	54%(16a''→18a'') + 46%(16a''→24a')
4A'	5.28	0.0026	87%(24a'→27a') + 9%(24a'→25a')				
5A'	5.39	0.0015	76%(16a''→17a'') + 12%(23a'→25a') + 9%(23a'→26a')	4A'	5.13	0.0140	37%(15a''→25a') + 34%(15a''→17a'') + 15%(23a'→26a')
6A'	5.44	0.0053	68%(23a'→25a') + 15%(23a'→26a') + 10%(23a'→27a')				
5A''	5.64	0.0001	100%(23a'→18a'')				
6A''	5.78	forbidden	60%(24a'→20a'') + 40%(24a'→19a'')				
7A'	5.81	0.0007	100%(24a'→28a')				
8A'	5.83	0.0104	88%(24a'→29a') + 12%(24a'→30a')				
9A'	5.89	0.0463	83%(24a'→30a') + 17%(24a'→29a')				
7A''	6.00	0.0335	68%(24a'→21a'') + 18%(24a'→22a'') + 10%(22a'→17a'')				
8A''	6.03	0.0058	47%(23a'→19a'') + 39%(23a'→20a'') + 11%(22a'→17a'')				
9A''	6.20	0.0035	41%(22a'→17a'') + 37%(16a''→26a') + 7%(23a'→20a'') + 6%(16a''→25a')				
10A'	6.27	0.0034	75%(24a'→31a') + 20%(23a'→27a')				
11A'	6.29	0.0080	58%(23a'→27a') + 27%(24a'→31a') + 6%(23a'→21a'') + 5%(15a''→17a'')				

^a Reference 42. ^b Notice that the SAC-CI assignments are not complete, as reported in ref 39.**Table 7.** Excitation Energies (eV), Oscillator Strengths, and Assignments Calculated with the LANL2DZ Pseudopotential on the Optimized Structure of MnO_4^-

TD-DFT/PBE0			SAC-CI ^a			experiment ^b		
excitation energy	oscillator strength	assignments	excitation energy	oscillator strength	assignments	excitation energy	oscillator strength	assignments
3.08	0.0095	89%(t ₁ →e) + 11%(t ₂ →e)	2.57	0.0202	t ₁ →e	2.27	strong (0.03)	t ₁ →e
4.31	0.0015	62%(t ₂ →e) + 38%(t ₁ →e)	3.58	0.0045	t ₁ →t ₂	3.47	weak	t ₁ →t ₂
4.84	0.0105	49%(t ₁ →t ₂) + 25%(t ₂ →e) + 16%(t ₂ →t ₂) + 8%(a ₁ →t ₂)	3.72	0.0136	t ₂ →e	3.99	strong (0.07)	t ₂ →e
6.42	0.0016	76%(t ₁ →t ₂) + 17%(t ₂ →e) + 7%(a ₁ →t ₂)	5.82	0.0022	t ₂ →t ₂ + a ₁ →t ₂	5.45	strong	t ₂ →t ₂
6.66	0.0017	50%(t ₂ →e) + 34%(a ₁ →t ₂) + 16%(t ₂ →t ₂)						

^a Reference 76. ^b Reference 77.

eV. One should notice that a fifth band around 6.5–7.0 eV is found but is neither reported in experimental records nor in other theoretical calculations.

Although they are consistent with the global behavior of the experimental spectrum, our results seem quite inaccurate. Furthermore, they are almost unaffected by the basis sets, as can be seen from the data of Table 8. Even basis sets including diffuse functions (SDD and Watchers) give large errors. Previous TD-DFT works give similar inaccuracy.^{60,66} Different explanations have been proposed for such a failure,

but the multiconfigurational nature of MnO_4^- seems the main cause.⁶⁰ This is well illustrated by the SAC-CI calculations,⁷⁶ whose results become more and more reliable as the active space increases. The energies listed in Table 7 come from an active space composed of 12 occupied and 41 empty orbitals. They are quite close to the experimental values, with a mean error of 0.26 eV.

To separate electronic from geometrical effects, we have carried out the same calculations on the experimental geometry ($d_{\text{Mn-O}} = 1.629 \text{ \AA}$). The results reported in Table

Table 8. Main Vertical Transitions (eV) of MnO_4^- with Different Basis Sets and Pseudopotentials^a

experimental structure			optimized structure		
excitation energy	oscillator strength	assignments	excitation energy	oscillator strength	assignments
LANL2DZ					
2.77	0.0077	$t_1 \rightarrow e$	3.08	0.0095	$t_1 \rightarrow e$
3.89	0.0007	$t_2 \rightarrow e$	4.31	0.0015	$t_2 \rightarrow e$; $t_1 \rightarrow t_2$
4.41	0.0099	$t_1 \rightarrow t_2$; $t_2 \rightarrow e$	4.84	0.0105	$t_1 \rightarrow t_2$
6.09	0.0044	$t_2 \rightarrow e$; $a_1 \rightarrow t_2$	6.42	0.0016	$t_1 \rightarrow t_2$
6.45	0.0041	$t_1 \rightarrow t_2$	6.66	0.0017	$t_2 \rightarrow e$; $a_1 \rightarrow t_2$
SBKJC					
2.82	0.0081	$t_1 \rightarrow e$	3.08	0.0097	$t_1 \rightarrow e$
3.95	0.0007	$t_2 \rightarrow e$	4.30	0.0015	$t_2 \rightarrow e$
4.46	0.0106	$t_2 \rightarrow e$	4.83	0.0112	$t_1 \rightarrow t_2$
6.16	0.0055	$a_1 \rightarrow t_2$	6.62	0.0045	$a_1 \rightarrow t_2$; $t_2 \rightarrow e$
			7.28	0.0281	$t_1 \rightarrow t_2$
SDD					
2.80	0.0077	$t_1 \rightarrow e$	3.13	0.0096	$t_1 \rightarrow e$
3.91	0.0009	$t_2 \rightarrow e$	4.35	0.0021	$t_2 \rightarrow e$
4.42	0.0100	$t_1 \rightarrow t_2$; $t_2 \rightarrow e$	4.89	0.0104	$t_1 \rightarrow t_2$
6.13	0.0079	$a_1 \rightarrow t_2$	6.68	0.0063	$t_2 \rightarrow e$
6.75	0.0051	$t_2 \rightarrow a_1$	6.79	0.0010	$a_1 \rightarrow a_1$; $t_2 \rightarrow a_1$
DZVP					
2.83	0.0081	$t_1 \rightarrow e$	3.06	0.0095	$t_1 \rightarrow e$
3.94	0.0007	$t_2 \rightarrow e$	4.25	0.0014	$t_2 \rightarrow e$
4.47	0.0108	$t_2 \rightarrow e$	4.80	0.0115	$t_2 \rightarrow e$; $t_1 \rightarrow t_2$
6.15	0.0045	$t_2 \rightarrow e$; $a_1 \rightarrow t_2$	6.59	0.0035	$t_2 \rightarrow e$; $a_1 \rightarrow t_2$
7.31	0.0299	$t_2 \rightarrow a_1$	7.80	0.1575	$e \rightarrow t_2$; $a_1 \rightarrow t_2$
Watchers + f					
2.84	0.0080	$t_1 \rightarrow e$	3.15	0.0098	$t_1 \rightarrow e$
3.96	0.0010	$t_2 \rightarrow e$	4.36	0.0023	$t_2 \rightarrow e$
4.48	0.105	$t_2 \rightarrow e$	4.92	0.0109	$t_1 \rightarrow t_2$
6.16	0.0048	$a_1 \rightarrow t_2$	6.71	0.0034	$t_2 \rightarrow e$; $a_1 \rightarrow t_2$
7.28	0.0498	$e \rightarrow t_2$	7.73	0.1242	$a_1 \rightarrow t_2$

^a Both results calculated with the experimental or with the PBE0 optimized structure are listed.

8 show a better agreement with the experimental values, even if the gap is still evident.

Finally, to verify the basis set effects on this difficult case, the only charged species in our set, we have carried out some calculations using the large 6-311++G(3df) basis for O and the LANL2DZ pseudopotential for Mn. Significant variations (around 0.2 eV) have been found, all the transition decreasing of about 0.2 eV. Nevertheless, the errors are still larger than in the other systems, thus clearly showing the predominant role of the multideterminant effects.

To sum up, the permanganate ion is a very complex system. The analysis of results is particularly difficult since values are altered by several parameters. Calculations on the X-ray structure point out the major role of correlation on the structural and spectroscopic parameters as well as the inherent defaults of the TD-DFT approach. When considering optimized structures, these inaccuracies are strengthened by geometrical problems.

4. Conclusion

We have investigated the optical excitations of four classes of transition-metal complexes in the framework of the time dependent DFT with the PBE0 hybrid functional. For each

system, excited states, oscillator strengths, and configurations have been analyzed in detail and compared to experimental and theoretical results so as to assess the effect of different basis sets (DZVP and Watchers + f) and pseudopotentials (LANL2DZ, SBKJC, and SDD) for the description of the metal.

The accurate calculation of charge transfer excitations remains a difficult task even though the combination of TD-DFT with hybrid functionals provides an satisfactory avenue to do so. Our results globally feature an absolute mean error in the order of 0.3–0.4 eV for most compounds. Largest discrepancies (up to 0.9 eV) have been found for the permanganate ion. In this case multiconfigurational effects underline a severe limit of the TD-DFT approach. All the same, these values are in the range of what is usually expected with TD-DFT.⁷² Corresponding intensities are much less affected and reproduce very well the experimental trends.

The effect of the basis set of the metal atoms turns out to be much more limited, the pseudopotentials being a more precise and convenient alternative to the all electron basis, even for first-row transition metals. Pseudopotentials can hence be recommended within the TD-DFT/PBE0 route and

represents a useful and fast tool for scientists for clarifying excitation processes of transition-metal complexes.

Supporting Information Available: Geometrical parameters (distances in Å and angles in deg) for optimized structures of CrF₆, MoF₆, WF₆, Ni(CO)₄, CpRh(CO)₂, CpIr(CO)₂, and MnO₄[−] (Table SI), excitation energies, oscillator strengths, and main configurations calculated on the PBE0 optimized structure of CrF₆ (SBKJC), MoF₆ (SDD), and WF₆ (LANL2DZ) (Table SII), and excitation energies, oscillator strengths, and main configurations calculated with the SDD pseudopotential on the PBE0 optimized structure of Ni(CO)₄ (Table SIII). This material is available free of charge via the Internet at <http://pubs.acs.org>.

References

- (1) Neese, F.; Zaleski, J. M.; Zaleski, K. L.; Solomon, E. I. *J. Am. Chem. Soc.* **2000**, *122*, 11703.
- (2) Petit, L.; Adamo, C.; Russo, N. *J. Phys. Chem. B* **2005**, *109*, 12214.
- (3) Ciofini, I.; Daul, C. A.; Adamo, C. *J. Phys. Chem. A* **2003**, *107*, 11182.
- (4) Koepke, C.; Wisniewski, K.; Grinberg, M.; Russell, D. L.; Holliday, K.; Beall, G. H. *J. Lumin.* **1998**, *78*, 135.
- (5) Koch, W.; Holthausen, M. C. *A Chemist's Guide to Density Functional Theory*; Wiley-VCH: Weinheim, Germany, 2000.
- (6) Adamo, C.; Barone, V. *Chem. Phys. Lett.* **2000**, *330*, 152.
- (7) Parac, M.; Grimme, S. *J. Phys. Chem. A* **2003**, *106*, 6844.
- (8) Yamaguchi, Y.; Yokoyama, S.; Mashiko, S. *J. Chem. Phys.* **2002**, *116*, 6541.
- (9) Ciofini, I.; Laine, P. P.; Bedioui, F.; Adamo, C. *J. Am. Chem. Soc.* **2004**, *126*, 10763.
- (10) Cavillot, V.; Champagne, B. *Chem. Phys. Lett.* **2002**, *354*, 449.
- (11) Van Caillie, C.; Amos, R. D. *Chem. Phys. Lett.* **1998**, *291*, 71.
- (12) Adamo, C.; Cossi, M.; Scalmani, G.; Barone, V. *Chem. Phys. Lett.* **1999**, *307*, 265.
- (13) Casida, M. E. In *Recent Advances in Density Functional Methods, Part I*; Chong, D. P., Ed.; World Scientific: Singapore, 1995.
- (14) Lainé, P. P.; Ciofini, I.; Ochsenbein, P.; Amouyal, E.; Adamo, C.; Bedioui, F. *Chem. Eur. J.* **2005**, *11*, 3711.
- (15) Tozer, D. J.; Handy, N. C. *Phys. Chem. Chem. Phys.* **2000**, *2*, 2117.
- (16) Dreuw, A.; Head-Gordon, M. *J. Am. Chem. Soc.* **2004**, *126*, 4007.
- (17) van Leeuwen, R.; Baerends, E. J. *Phys. Rev. A* **1994**, *49*, 2421.
- (18) Gritsenko, O.; Baerends, J. *Chem. Phys.* **2004**, *121*, 655.
- (19) Tozer, D. J.; Handy, N. C. *J. Chem. Phys.* **1998**, *109*, 10180.
- (20) Ernzerhof, M.; Scuseria, G. E. *J. Chem. Phys.* **1999**, *109*, 911.
- (21) Adamo, C.; Barone, V. *J. Chem. Phys.* **1999**, *110*, 6158.
- (22) Adamo, C.; Barone, V. *Theor. Chem. Acc.* **2000**, *105*, 169.
- (23) Aquilante, F.; Cossi, M.; Crescenzi, O.; Scalmani, G.; Barone, V. *Mol. Phys.* **2003**, *101*, 1945.
- (24) Adamo, C.; Scuseria, G. E.; Barone, V. *J. Chem. Phys.* **1999**, *111*, 2889.
- (25) Adamo, C.; Barone, V. *Chem. Phys. Lett.* **1999**, *314*, 152.
- (26) Bernasconi, L.; Blumberger, J.; Sprik, M.; Vuilleumier, R. *J. Chem. Phys.* **2004**, *121*, 11885.
- (27) Perdew, J. P.; Burke, K.; Ernzerhof, M. *Phys. Rev. Lett.* **1996**, *77*, 3865, **1997**, *78*, 1396.
- (28) Wiberg, K. B.; De Oliveira, A. E.; Trucks, G. J. *Phys. Chem. A* **2002**, *106*, 4192.
- (29) Broclawok, E.; Borowski, T. *Chem. Phys. Lett.* **2001**, *339*, 433.
- (30) Wiberg, K. B. *J. Comput. Chem.* **2004**, *25*, 1342.
- (31) Monat, J.; Rodriguez, J. H.; McCusker, J. K. *J. Phys. Chem. A* **2002**, *106*, 7399.
- (32) Gaussian 03, Revision B. 05. Frisch, M. J.; Trucks, G. W.; Schlegel, H. B.; Scuseria, G. E.; Robb, M. A.; Cheeseman, J. R.; Montgomery, J. A., Jr.; Vreven, T.; Kudin, K. N.; Burant, J. C.; Millam, J. M.; Iyengar, S. S.; Tomasi, J.; Barone, V.; Mennucci, B.; Cossi, M.; Scalmani, G.; Rega, N.; Petersson, G. A.; Nakatsuji, H.; Hada, M.; Ehara, M.; Toyota, K.; Fukuda, R.; Hasegawa, J.; Ishida, M.; Nakajima, T.; Honda, Y.; Kitao, O.; Nakai, H.; Klene, M.; Li, X.; Knox, J. E.; Hratchian, H. P.; Cross, J. B.; Bakken, V.; Adamo, C.; Jaramillo, J.; Gomperts, R.; Stratmann, R. E.; Yazyev, O.; Austin, A. J.; Cammi, R.; Pomelli, C.; Ochterski, J. W.; Ayala, P. Y.; Morokuma, K.; Voth, G. A.; Salvador, P.; Dannenberg, J. J.; Zakrzewski, V. G.; Dapprich, S.; Daniels, A. D.; Strain, M. C.; Farkas, O.; Malick, D. K.; Rabuck, A. D.; Raghavachari, K.; Foresman, J. B.; Ortiz, J. V.; Cui, Q.; Baboul, A. G.; Clifford, S.; Cioslowski, J.; Stefanov, B. B.; Liu, G.; Liashenko, A.; Piskorz, P.; Komaromi, I.; Martin, R. L.; Fox, D. J.; Keith, T.; Al-Laham, M. A.; Peng, C. Y.; Nanayakkara, A.; Challacombe, M.; Gill, P. M. W.; Johnson, B.; Chen, W.; Wong, M. W.; Gonzalez, C.; Pople, J. A.; Gaussian, Inc., Wallingford CT, 2004.
- (33) Stratmann, R. E.; Scuseria, G. E.; Frisch, M. J. *J. Chem. Phys.* **1998**, *109*, 8128.
- (34) Hedberg, L.; Iijima, T.; Hedberg, K. *J. Chem. Phys.* **1979**, *70*, 3224.
- (35) Brockway, L. O.; Cross, P. C. *J. Chem. Phys.* **1935**, *3*, 828.
- (36) Palenik, G. J. *Inorg. Chem.* **1967**, *6*, 503.
- (37) Russo, T. V.; Martin, R. L.; Hay, P. J. *J. Chem. Phys.* **1995**, *102*, 8023.
- (38) Gillespie, R. J.; Bytheway, I.; Tang, T. H.; Bader, R. W. *Inorg. Chem.* **1996**, *35*, 3954.
- (39) Quinones, G. S.; Hägele, G.; Seppelt, K. *Chem. Eur. J.* **2004**, *10*, 4755.
- (40) Marsden, C. J.; Moncrieff, D.; Quelch, G. E. *J. Phys. Chem.* **1994**, *98*, 2038.
- (41) Tanpipat, N.; Baker, J. *J. Phys. Chem.* **1996**, *100*, 19818.
- (42) Hu, Z.; Boyd, R. J.; Nakatsuji, H. *J. Am. Chem. Soc.* **2002**, *124*, 2664.
- (43) Hay, P. J.; Wadt, W. R. *J. Chem. Phys.* **1985**, *82*, 284.
- (44) Ortiz, J. V.; Hay, P. J.; Martin, R. L. *J. Am. Chem. Soc.* **1992**, *114*, 2736.

- (45) Stevens, W. J.; Krauss, M.; Basch, H.; Jasien, P. G. *Can. J. Chem.* **1992**, *70*, 612.
- (46) Dolg, M.; Wedig, U.; Stoll, H.; Preuss, H. *J. Chem. Phys.* **1987**, *86*, 866.
- (47) Andrae, D.; Haeussermann, U.; Dolg, M.; Stoll, H.; Preuss, H. *Theor. Chim. Acta* **1990**, *77*, 123.
- (48) Wachters, A. J. H. *J. Chem. Phys.* **1970**, *52*, 1033.
- (49) Bauschlicher, C. W.; Langhoff, S. R., Jr.; Barnes, L. A. *J. Chem. Phys.* **1989**, *91*, 2399.
- (50) Chiodo, N. S.; Russo, N.; Sicilia, E. *J. Comput. Chem.* **2005**, *26*, 175.
- (51) Godbout, N.; Salahub, D. R.; Andzelm, J.; Wimmer, E. *Can. J. Chem.* **1992**, *70*, 560.
- (52) Daniel, C. *Coord. Chem. Rev.* **2003**, *238–239*, 143.
- (53) Marsden, C. J.; Wolyne, P. P. *Inorg. Chem.* **1991**, *30*, 1682.
- (54) Hope, E. G.; Levason, W.; Ogden, J. S. *Inorg. Chem.* **1991**, *30*, 4873.
- (55) Pierloot, K.; Roos, B. O. *Inorg. Chem.* **1992**, *31*, 5353.
- (56) Hope, E. G.; Jones, P. J.; Levason, W.; Ogden, J. S.; Tajik, M.; Turff, J. W. *J. Chem. Soc., Dalton Trans.* **1985**, 1443.
- (57) McDiarmid, R. *J. Chem. Phys.* **1974**, *61*, 3333.
- (58) Nakai, H.; Morita, H.; Tomasello, P.; Nakatsuji, H. *J. Phys. Chem. A* **1998**, *102*, 2033.
- (59) Bloor, J. E.; Sherrod, R. E. *J. Am. Chem. Soc.* **1980**, *102*, 4333.
- (60) Boulet, P.; Chermette, H.; Daul, C.; Gilardoni, F.; Rogemont, F.; Weber, J.; Zuber, G. *J. Phys. Chem. A* **2001**, *105*, 885.
- (61) Schreiner, A. F.; Brown, T. L. *J. Am. Chem. Soc.* **1968**, *90*, 3366.
- (62) Lever, A. B. P.; Ozin, G. A.; Halan, A. J. L.; Power, W. J.; Gray, H. B. *Inorg. Chem.* **1979**, *18*, 2088.
- (63) Kotzian, M.; Rösch, N.; Schröder, H.; Zerner, M. C. *J. Am. Chem. Soc.* **1989**, *111*, 7687.
- (64) Pierloot, K.; Tsokos, E.; Vanquickenborne, L. G. *J. Phys. Chem.* **1996**, *100*, 16545.
- (65) Hada, M.; Imai, Y.; Hidaka, M.; Nakatsuji, H. *J. Phys. Chem.* **1995**, *103*, 6993.
- (66) Gisbergen, S. J. A.; Groeneveld, J. A.; Rosa, A.; Snijders, J. G.; Baerends, E. J. *J. Phys. Chem. A* **1999**, *103*, 6835.
- (67) Rösch, N.; Jörg, H.; Kotzian, M. *J. Chem. Phys.* **1987**, *86*, 4038.
- (68) Nooijen, M.; Lotrich, V. *J. Chem. Phys.* **2000**, *113*, 494.
- (69) Dunwoody, N.; Lees, A. J. *Organometallics* **1997**, *16*, 5770.
- (70) Hoyano, J. K.; Graham, W. A. *J. Am. Chem. Soc.* **1982**, *104*, 3723.
- (71) Hoyano, J. K.; McMaster, A. D.; Graham, W. A. *J. Am. Chem. Soc.* **1983**, *105*, 7190.
- (72) Purwoko, A. A.; Drolet, D. P.; Lees, A. J. *J. Organomet. Chem.* **1995**, *504*, 107.
- (73) Hay, P. J.; Wadt, W. R. *J. Chem. Phys.* **1985**, *82*, 270.
- (74) Atananov, M.; Brunold, T. C.; Güdel, H. U.; Daul, D. *Inorg. Chem.* **1998**, *37*, 4789.
- (75) Johansen, H.; Rettrup, S. *Mol. Phys.* **1983**, *49*, 1209.
- (76) H. Nakai, H.; Ohmori, Y.; Nakatsuji, H. *J. Chem. Phys.* **1991**, *95*, 8287.
- (77) Holt, L.; Balhausen, C. *Theor. Chim. Acta* **1967**, *7*, 313.

CT0500500